



Research article

Supervised neural learning for the predator-prey delay differential system of Holling form-III

Naret Ruttanaprommarin¹, Zulqurnain Sabir^{2,3}, Salem Ben Said², Muhammad Asif Zahoor Raja⁴, Saira Bhatti⁵, Wajaree Weera⁶ and Thongchai Botmart^{6,*}

¹ Department of Science and Mathematics, Faculty of Industry and Technology, Rajamangala University of Technology Isan Sakonnakhon Campus, Sakonnakhon 47160, Thailand

² Department of Mathematical Sciences, United Arab Emirates University, P.O. Box 15551, Al Ain, UAE

³ Department of Mathematics, Hazara University, Mansehra, Pakistan

⁴ Future Technology Research Center, National Yunlin University of Science and Technology, 123 University Road, Section 3, Douliou, Yunlin 64002, Taiwan

⁵ Department of Mathematics, COMSATS University Islamabad, Abbottabad Campus, Abbottabad Pakistan

⁶ Department of Mathematics, Faculty of Science, Khon Kaen University, Khon Kaen 40002, Thailand

* **Correspondence:** Email: thongbo@kku.ac.th.

Abstract: The purpose of this work is to present the stochastic computing study based on the artificial neural networks (ANNs) along with the scaled conjugate gradient (SCG), ANNs-SCG for solving the predator-prey delay differential system of Holling form-III. The mathematical form of the predator-prey delay differential system of Holling form-III is categorized into prey class, predator category and the recent past effects. Three variations of the predator-prey delay differential system of Holling form-III have been numerical stimulated by using the stochastic ANNs-SCG procedure. The selection of the data to solve the predator-prey delay differential system of Holling form-III is provided as 13%, 12% and 75% for testing, training, and substantiation together with 15 neurons. The correctness and exactness of the stochastic ANNs-SCG method is provided by using the comparison of the obtained and data-based reference solutions. The constancy, authentication, soundness, competence, and precision of the stochastic ANNs-SCG technique is performed through the analysis of the correlation measures, state transitions (STs), regression analysis, correlation, error histograms (EHs) and MSE.

Keywords: time delay; Holling form-III; mathematical system; artificial neural networks; scaled conjugate gradient

Mathematics Subject Classification: 92B20, 34A34

1. Introduction

The predator-prey interactions perform the major evolution that is used to consider the mechanisms effects in terms of the population's collaboration based on the ecological civilizations. Many scientists have constructed the mathematical systems using the inspirations of the population of the predator into the prey together with the ecology form of the density conditions. Numerous predator-prey models represent the predator's growth that is directly related to the density of the prey together and vice versa. The growth of the prey is directly related to the predator density with the current time. It is predictable that the growth of the predator depends upon the density of the prey in the present and the recent past [1,2]. Therefore, the biological influences are more realistic to perform the fading impacts of the memory. Some relevant recent studies based on the past prey density using the predator-prey interactions are discussed in [3–6].

The Allee effects defined by Allee provide the positive impacts based on the correlation between the precise fitness and population size [7–12]. Most of the relations based on the predator-prey are assumed to the growth of the logistic prey. The Allee impacts using the dynamics of the prey signify the population problems, genetic drift, including insufficient alimentation at low densities, inbreeding depression, mate restriction, predator evading of resistance [13–17]. Therefore, the Allee effects are provided as a serious factor based on the biological controller and commonly improves the loss prospect of the individual [18]. These impacts can be applied to indicate the weak and strong ratio based on the growth. The strong Allee's impacts [19–21] provide the growth (positive) ratio per capita, whereas the weak Allee effects indicate the growth rate (negative) per capita. The occurrence of Allee effects has already been provided in numerous biological individuals, like as marine invertebrates (gastropod) [22], mammals (suricates) [23], and insects (Glanville Fritillary butterfly) [24].

Few of the transition states cannot be prompt and the predator-prey interactions based on the time delay systems have achieved huge significance over the last few years [25–27]. The natural population dynamics indicates the reliability that is associated with the species response. On the constancy of the population, there are various factors of the time delay [28,29]. Subsequently, the time delay factor is applied in diverse ordinary form of the differential models that can be provided more accurate form. Few of the models based on the time delay factors indicate the destabilization of the model using the accompaniment of the Hopf bifurcation with the strong oscillation dynamics [30,31]. There are a few investigations in the literature that have been presented based on the Allee effects, which makes the system stable with the delay factors [32]. The biological models, cooperation and competition are associated with the population dynamics along with the factor of time delay. The competition of the population usually rises based on the food, whereas the collaboration in the population normally indicates to assume the prey or to avoid from the predator.

The aim of such investigations is to present the numerical performances through the artificial neural networks (ANNs) along with the scaled conjugate gradient (SCG), ANNs-SCG for solving the predator-prey delay differential system of Holling form-III. The predator-prey dynamics along with the delay factors in the prey competition/cooperation using the Allee effects with fading memory has

never been presented before through the ANNs-SCG technique. The stochastic based computational investigations have been presented in this study to solve various complex and complicated types of dynamical systems. To mention some of them are HIV dynamical models [33], a food chain system of models [34,35], coronavirus dynamical systems [36], differential form of the eye surgery model [37,38], singular thermal explosion theory model [39], singular differential models [40], and nonlinear smoking differential system [41]. Few novel features of the proposed stochastic study are indicated as:

- The design of the predator-prey delay differential system with Holling form-III based on two delay terms, cooperation/competition dynamics and the prey Allee effects is presented.
- The numerical performances of the predator-prey delay differential system with Holling form-III are provided by using the stochastic procedures of the ANNs-SCG solver.
- Three different variations based on the predator-prey delay differential system with Holling form-III are provided have been performed numerically through the ANNs-SCG solver.
- The correctness of the ANNs-SCG computing solver is performed by using the relative performances of the achieved and the reference results.
- The dependability and consistency of the ANNs-SCG computing solver is approved through the absolute error (AE) value for solving the predator-prey delay differential system with Holling form-III.
- The STs, regression values, MSE performances, EHs and correlation measures are provided using the ANNs-SCG computing for solving the predator-prey delay differential system with Holling form-III.

The paper is organized as: Section 2 shows the mathematical formulation of the predator-prey delay differential system with Holling form-III. The designed structure is given in Section 3, whereas Section 4 shows the result simulations. Concluding remarks are presented in the final section.

2. Mathematical formulations of the model

In this section, the design of the predator-prey delay differential system based Holling form-III with two delay terms, cooperation/competition dynamics and the prey Allee effects is provided. The density of the predator consists of the past and present populations of the prey. In this model, the competition delay form shows the instability, however the delay term induces the stability based on the Hopf bifurcation. The fading state based on the memory term is considered by considering the growth rate of the predator. Hence a biological model using the growth rate of the predator species is provided along with the prey density. The functional response of the predator using the predator-prey interactions has been established in four factors based on the Holling type I–IV. The Holling form III designates the functional response of the predation positive impacts that relate to the population of prey. The predation impacts increase in the enhancement of the prey population. These forms of responses are usually considered when the predator competently achieves a substitute source with low prey density. There are various studies using the Allee effects have been provided together with Holling form III and the functional response [42–44]. The predator-prey delay differential mathematical system based Holling form-III based on two delay terms is given as [45]:

$$\begin{cases} \frac{dP(y)}{dy} = \psi P(y) \left(1 - \frac{P_{y_1}}{k}\right) (P_{y_1} - h) - \frac{b(P(y))^2 Q(y)}{d + (P(y))^2} & P(0) = \phi_1, \\ \frac{dQ(y)}{dy} = \frac{sbR(y)^2 Q(y)}{d + (R(y))^2} - \tau Q(y) - m(Q(y))^2 & Q(0) = \phi_2, \\ \frac{dR(y)}{dy} = \frac{1}{\delta} (P(y) - R(y)) & R(0) = \phi_3, \end{cases} \quad (1)$$

in the above model, $P_{y_1} = P(y-t_1)$ and $P_{y_2} = P(y-t_2)$ represent the time delay forms of the predator-prey delay differential system and the parameter descriptions are shown in Table 1.

Table 1. Detailed parameters using the proposed ANNs-SCG procedure for the predator-prey delay differential system of Holling form-III.

Parameter	Values
$P(y)$	Prey
$Q(y)$	Predator
$R(y)$	Secluded number of characters
d	Rate of development from $P(y)$ to $Q(y)$
b	Growth of natural population
ψ	Development term
τ	Rate of development from $P(y)$ to $R(y)$, cure of secluded characters
m	Rate of development from $P(y)$ to $R(y)$, cure of diseased characters
t_1	Delay element
y	Period
t_2	Delay element
\mathcal{S}	Qualities' death rate
ϕ_1, ϕ_2, ϕ_3	Opening conditions

3. Proposed ANNs-SCG procedure

This part of the research provides the ANNs-SCG procedure for solving the predator-prey delay differential system of Holling form-III is provided by the significant operators based on the proposed stochastic ANNs-SCG and the implemented procedures of the stochastic ANNs-SCG scheme. The simulations of three different cases of the predator-prey delay differential system of Holling form-III are provided by using the ANNs-SCG procedure. Fifteen neurons have been used to solve the predator-prey delay differential system of Holling form-III along with the selection of data chosen as 13%, 12% and 75% for testing, training, and substantiation. The structure of the input, hidden and output layers is provided in Figure 1, while the optimization procedures using the multi-layer ANNs-SCG technique are given in Figure 2.

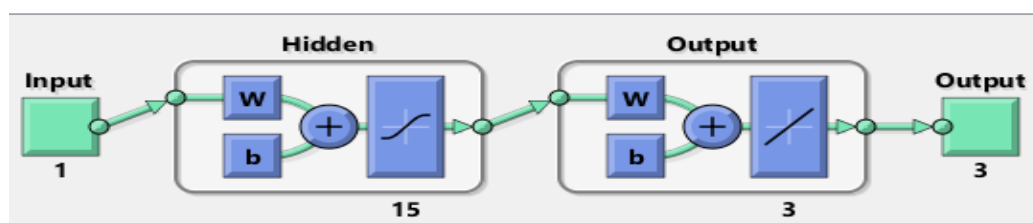


Figure 1. Input, Hidden and output layer procedure for the predator-prey delay differential system of Holling form-III.

1. Model: predator-prey delay differential system

Stochastic computing method

A multi-layer process is constructed through the stochastic computing study based on the artificial neural networks (ANNs) along with the scaled conjugate gradient (SCG), ANNs-SCG for solving the predator-prey delay differential system of Holling form-III

$$\begin{cases} \frac{dP(y)}{dy} = \psi P(y) \left(1 - \frac{P_{y_1}}{k}\right) (P_{y_1} - h) - \frac{b(P(y))^2 Q(y)}{d + (P(y))^2} & P(0) = \phi_1, \\ \frac{dQ(y)}{dy} = \frac{sbR(y)^2 Q(y)}{d + (R(y))^2} - \tau Q(y) - m(Q(y))^2 & Q(0) = \phi_2, \\ \frac{dR(y)}{dy} = \frac{1}{\delta} (P(y) - R(y)) & R(0) = \phi_3, \end{cases}$$

Mathematical formulation

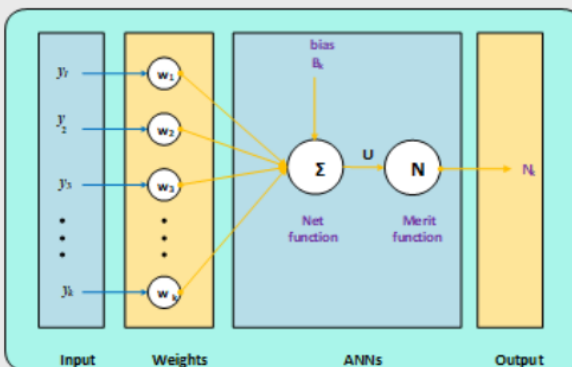
2. Methodology: ANNs-SCG

Reference dataset

The Runge-Kutta numerical scheme is used to perform the numerical simulations of the predator-prey delay differential system of Holling form-III

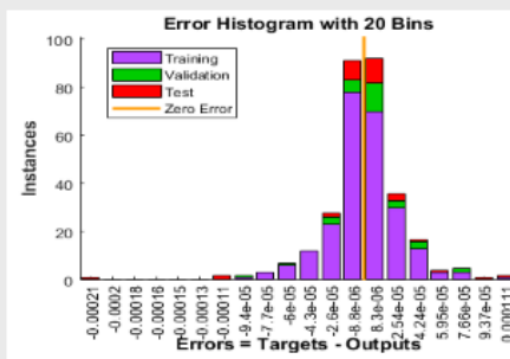
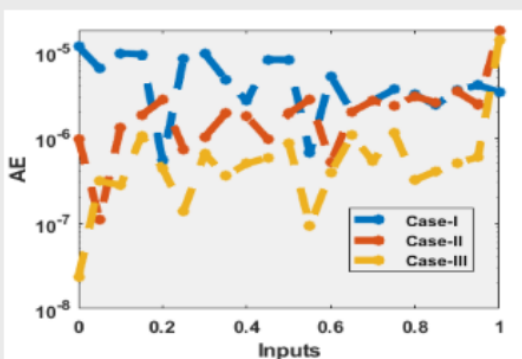
Achieved performances

Simulations through the stochastic computing ANNs-SCG approach using the reference statics to authenticate the approximate simulations of the of the predator-prey delay differential system of Holling form-III



A single neuron network

3. Results



Proposed outcomes via ANNs-SCG scheme through the EHs, STs, MSE, regressions and fitness and to perform the numerical simulations of the predator-prey delay differential system of Holling form-III

Figure 2. Designed ANNs-SCG procedure for solving the predator-prey delay differential system of Holling form-III.

4. Simulation of the results

This section shows the numerical performances of three different cases based on the predator-prey delay differential system of Holling form-III by using the ANNs-SCG procedure. The mathematical representation of each case is provided as:

Case 1: Consider the predator-prey delay differential system of Holling form-III with $b=0.4$, $d=0.14$, $\delta=0.21$, $t_1=0.11$, $t_2=0.15$, $s=0.41$, $m=0.7$, $h=0.3$, $\tau=0.6$, $k=0.1$, $\psi=0.2$, $\phi_1=0.15$, $\phi_2=0.2$ and $\phi_3=0.25$.

$$\begin{cases} \frac{dP(y)}{dy} = 0.2P(y) \left(1 - \frac{P(y-0.11)}{0.1} \right) (P(y-0.15) - 0.3) - \frac{0.4(P(y))^2 Q(y)}{0.14 + (P(y))^2} & P(0) = 0.15, \\ \frac{dQ(y)}{dy} = \frac{0.16(R(y))^2 Q(y)}{0.14 + (R(y))^2} - 0.6Q(y) - 0.7(Q(y))^2 & Q(0) = 0.2, \\ \frac{dR(y)}{dy} = 4.76(P(y) - R(y)) & R(0) = 2.5. \end{cases} \quad (3)$$

Case 2: Consider the predator-prey delay differential system of Holling form-III with $b=0.4$, $d=0.14$, $\delta=0.21$, $t_1=0.11$, $t_2=0.15$, $s=0.41$, $m=0.7$, $h=0.3$, $\tau=0.6$, $k=0.1$, $\psi=0.2$, $\phi_1=0.2$, $\phi_2=0.25$ and $\phi_3=0.25$:

$$\begin{cases} \frac{dP(y)}{dy} = 0.2P(y) \left(1 - \frac{P(y-0.11)}{0.1} \right) (P(y-0.15) - 0.3) - \frac{0.4(P(y))^2 Q(y)}{0.14 + (P(y))^2} & P(0) = 0.2, \\ \frac{dQ(y)}{dy} = \frac{0.16(R(y))^2 Q(y)}{0.14 + (R(y))^2} - 0.6Q(y) - 0.7(Q(y))^2 & Q(0) = 0.25, \\ \frac{dR(y)}{dy} = 4.76(P(y) - R(y)) & R(0) = 0.3. \end{cases} \quad (4)$$

Case 3: Consider the predator-prey delay differential system of Holling form-III with $b=0.4$, $d=0.14$, $\delta=0.21$, $t_1=0.11$, $t_2=0.15$, $s=0.41$, $m=0.7$, $h=0.3$, $\tau=0.6$, $k=0.1$, $\psi=0.2$, $\phi_1=0.2$, $\phi_2=0.25$ and $\phi_3=0.25$:

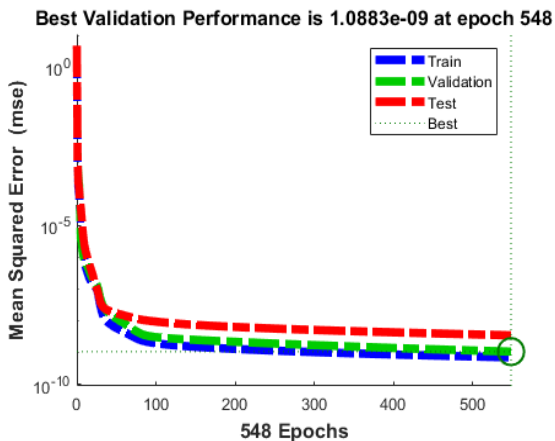
$$\begin{cases} \frac{dP(y)}{dy} = 0.2P(y) \left(1 - \frac{P(y-0.11)}{0.1} \right) (P(y-0.15) - 0.3) - \frac{0.4(P(y))^2 Q(y)}{0.14 + (P(y))^2} & P(0) = 0.25, \\ \frac{dQ(y)}{dy} = \frac{0.16(R(y))^2 Q(y)}{0.14 + (R(y))^2} - 0.6Q(y) - 0.7(Q(y))^2 & Q(0) = 0.3, \\ \frac{dR(y)}{dy} = 4.76(P(y) - R(y)) & R(0) = 0.35. \end{cases} \quad (5)$$

The numerical results based on the predator-prey delay differential system of Holling form-III using the stochastic ANNs-SCG procedure are presented in Figures 3–5. Figure 3 indicates the gradient

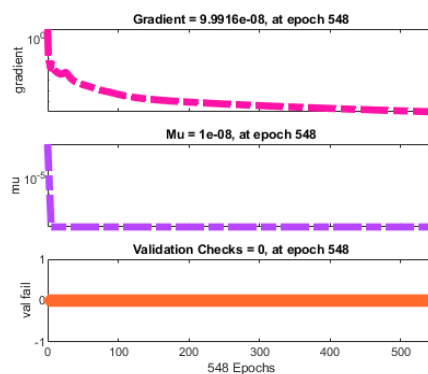
measures and best assessments performances for solving the predator-prey delay differential system of Holling form-III. These plots show the STs and MSE performances of the best curves, training and verification to solve three different cases of the predator-prey delay differential system of Holling form-III. The obtained performances based on the predator-prey delay differential system have been provided using the iterations 548, 48 and 39 that are calculated as 1.0883×10^{-9} , 4.312×10^{-10} and 4.669×10^{-10} , respectively. The gradient values are also reported in Figure 3 for solving the predator-prey delay differential system. These gradient performances are reported as 9.9916×10^{-8} , 9.51×10^{-8} and 9.3259×10^{-8} for the predator-prey delay differential system. The graphical plots represent the convergence performances of the ANNs-SCG stochastic technique to solve the predator-prey delay differential system. Figure 4 signifies the performances of the fitting cures for solving the predator-prey delay differential system. These graphical representations indicate the result comparisons for each variation of the predator-prey delay differential system. The error plots representations using the validation, testing, and training have been provided for each variation of the predator-prey delay differential system using the ANNs-SCG solver. The EHs plots together with the regression measures are provided in Figure 4 for the predator-prey delay differential system using the ANNs-SCG solver. The values of the EHs have been reported as 8.3×10^{-6} , 5.3×10^{-6} and 5.7×10^{-6} for the respective variations of the predator-prey delay differential system. The plots based on the regression measures have been derived in Figure 5 to signify the correlation values. It is noted that the correlation performances are reported as 1 for the respective variations of the predator-prey delay differential system using the ANNs-SCG solver. The authentication, testing and training performances signify the accuracy and exactness of the ANNs-SCG technique to solve the predator-prey delay differential system using the ANNs-SCG solver. The MSE measures via training, testing, verification, complexity, epochs, and backpropagation are provided in Table 2 for the predator-prey delay differential system using the ANNs-SCG solver.

Table 2. Proposed ANNs-SCG technique for the predator-prey delay differential system.

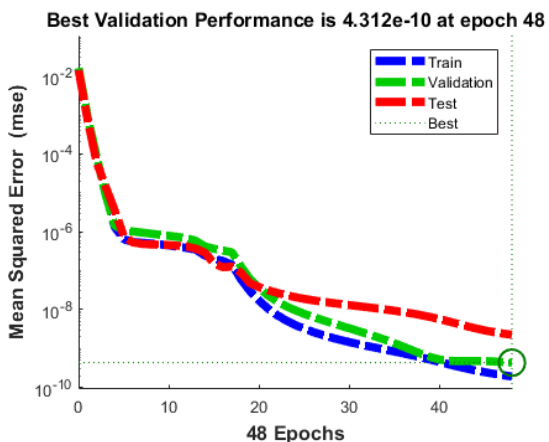
Case	MSE			Gradient	Mu	Iterations	Performance	Time
	Testing	Training	Endorsement					
1	3×10^{-9}	7.16×10^{-10}	1.08×10^{-9}	9.99×10^{-8}	1.00×10^{-10}	548	7.17×10^{-10}	04
2	2×10^{-9}	1.90×10^{-10}	4.312×10^{-10}	9.51×10^{-8}	1.00×10^{-10}	48	1.90×10^{-10}	02
3	2×10^{-11}	7.36×10^{-12}	4.66×10^{-10}	9.33×10^{-8}	1.00×10^{-9}	39	7.37×10^{-12}	01



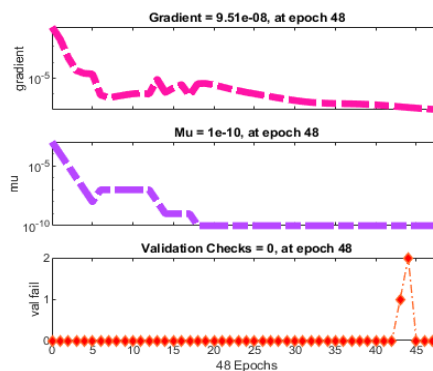
(a) Case 1 MSE



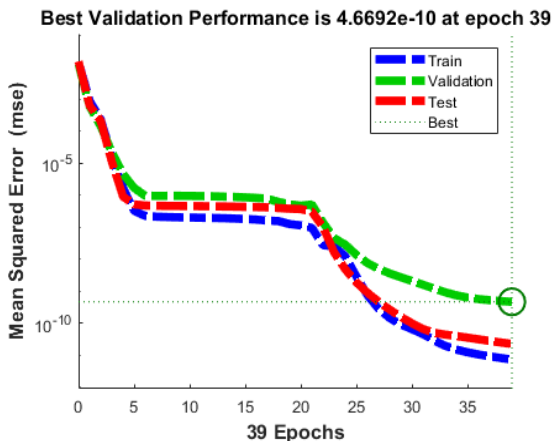
(a) Case I: STs



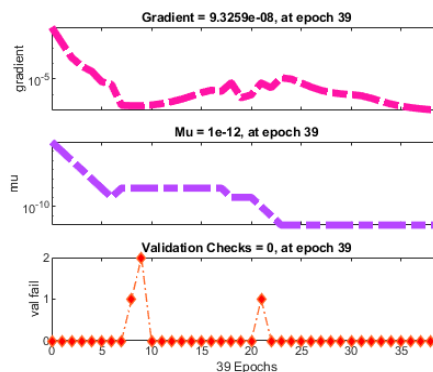
(b) Case 2: MSE



(b) Case 2: STs

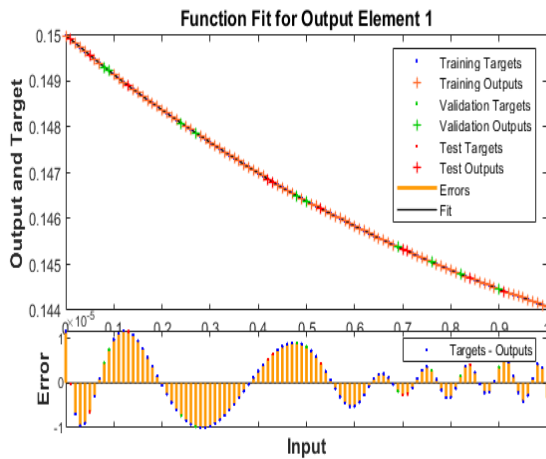


(c) Case 3: MSE

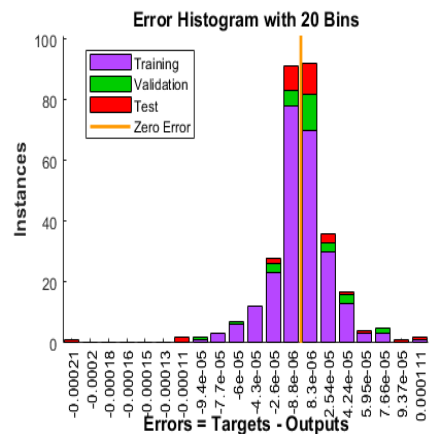


(c) Case 3: STs

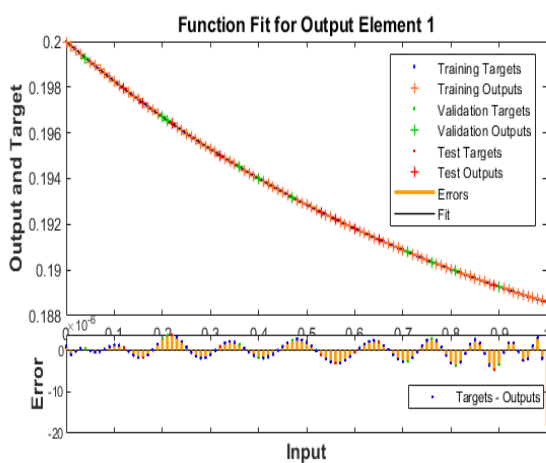
Figure 3. MSE and STs for the predator-prey delay differential system using the ANNs-SCG solver.



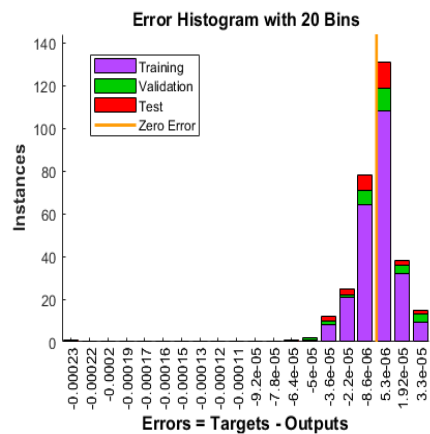
(a) Case 1 Results



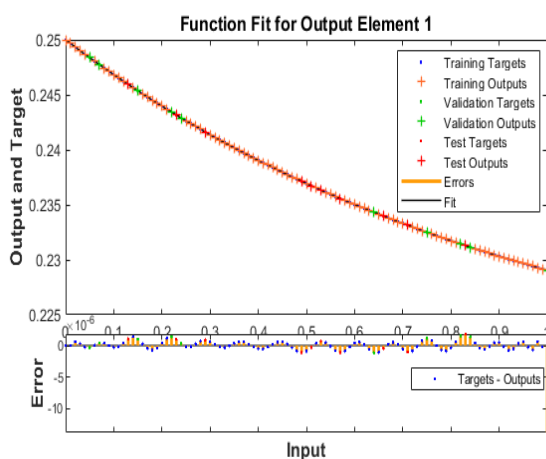
(a) Case I: EHs



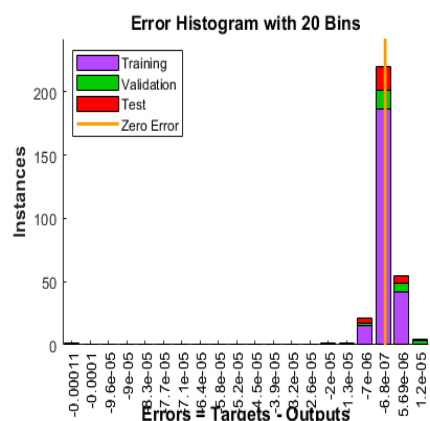
(b) Case 2: Results



(b) Case 2: EHs

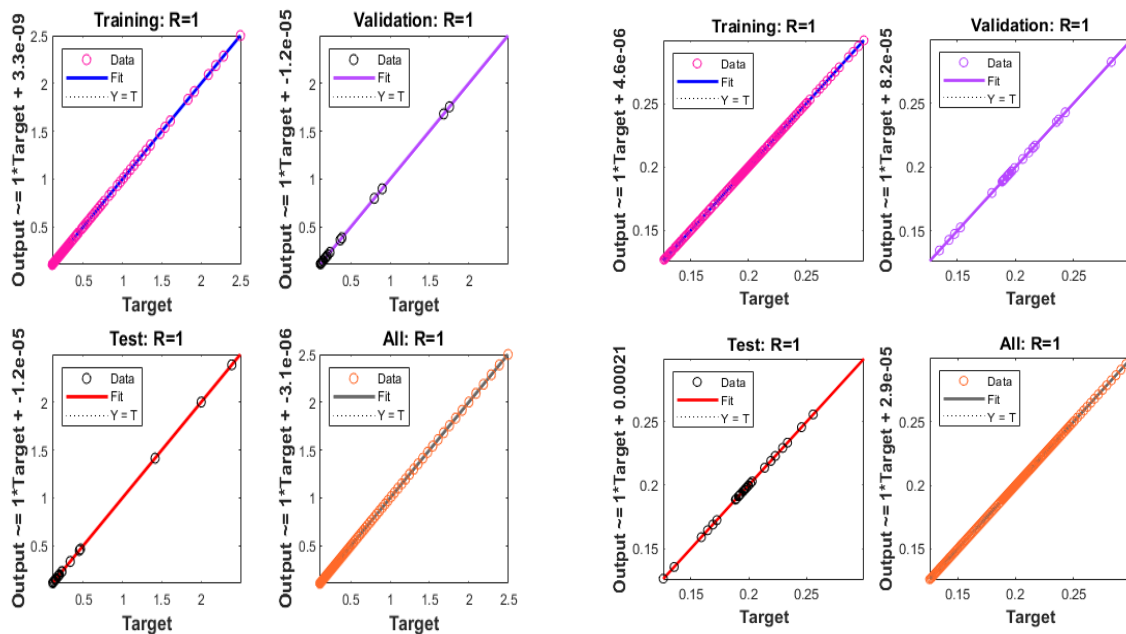


(c) Case 3: Results



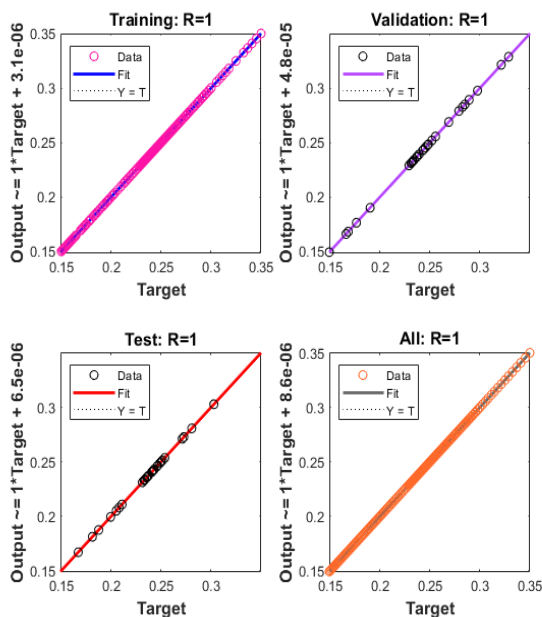
(c) Case 3: EHs

Figure 4. EHs and result performances for the predator-prey delay differential system using the ANNs-SCG solver.



(a) Regression: Case 1

(b) Regression: Case 2



(c) Regression: Case 3

Figure 5. Regression measures based on the predator-prey delay differential system using the ANNs-SCG solver.

The result comparison performances and the values of the AE are provided for three different cases of the predator-prey delay differential system using the ANNs-SCG solver is presented in Figures 6 and 7. The precision of the results based on the stochastic ANNs-SCG technique is provided in Figure 6 for solving the predator-prey delay differential system of Holling form-III. The overlapping of the results is performed for solving the predator-prey delay differential system of Holling form-III. The performances of the AE based on the ANNs-SCG computing solver for three different cases of the predator-prey delay differential system of Holling form-III is signified in Figure 7. The predator-prey delay differential system of Holling form-III is classified into three dynamics, $P(y)$, $Q(y)$ and $R(y)$. The AE for $P(y)$ is performed as 10^{-5} to 10^{-6} , 10^{-5} to 10^{-7} and 10^{-6} to 10^{-8} for the respective cases of the predator-prey delay differential system. The AE performances for the $Q(y)$ category is presented as 10^{-4} to 10^{-5} , 10^{-3} to 10^{-5} and 10^{-4} to 10^{-6} for the delay differential system. The AE measures for $R(y)$ class is presented as 10^{-4} to 10^{-5} , 10^{-3} to 10^{-5} and 10^{-4} to 10^{-6} for the respective cases of the predator-prey delay differential system.

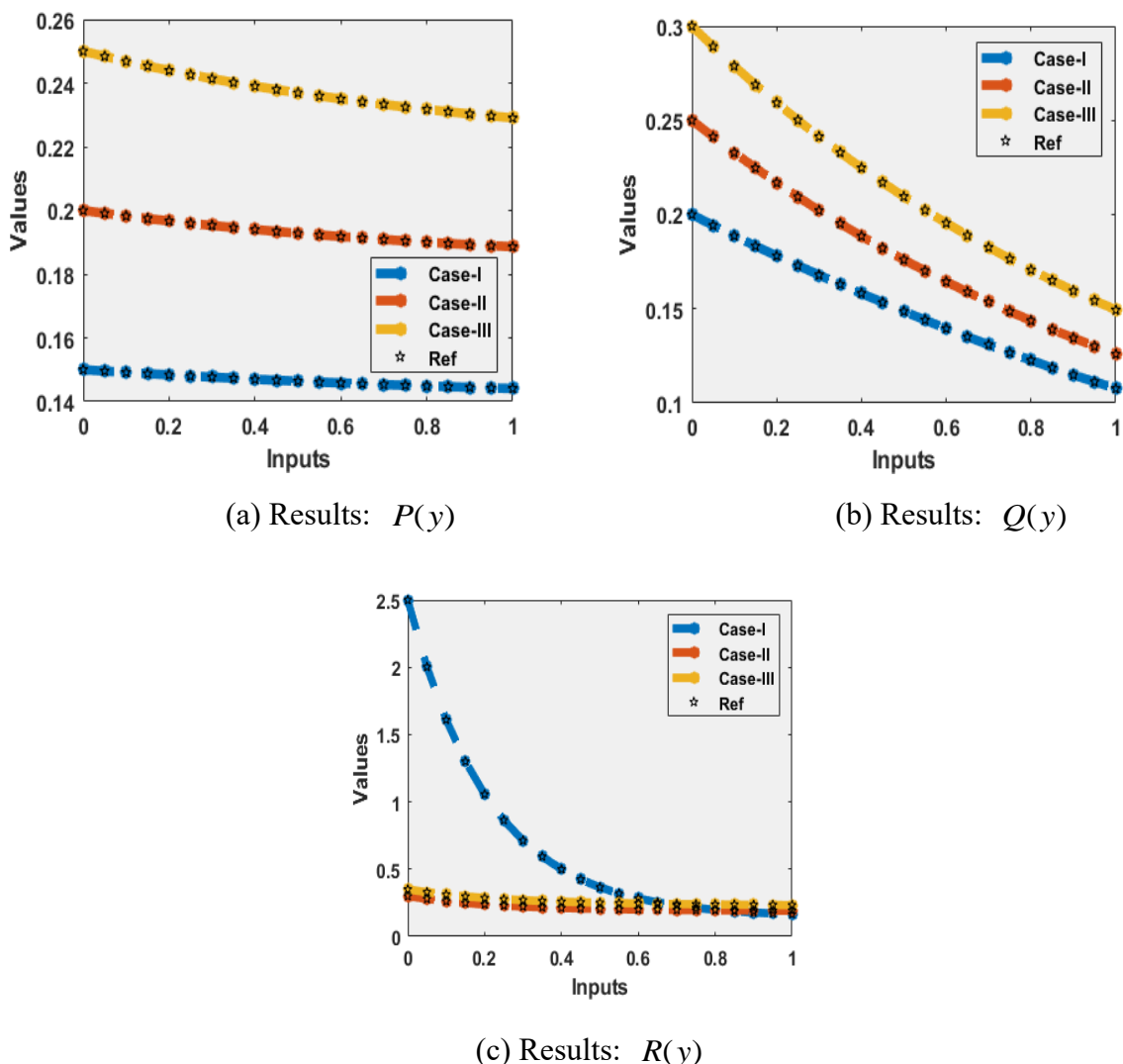


Figure 6. Results comparisons for the predator-prey delay differential system using the ANNs-SCG solver.

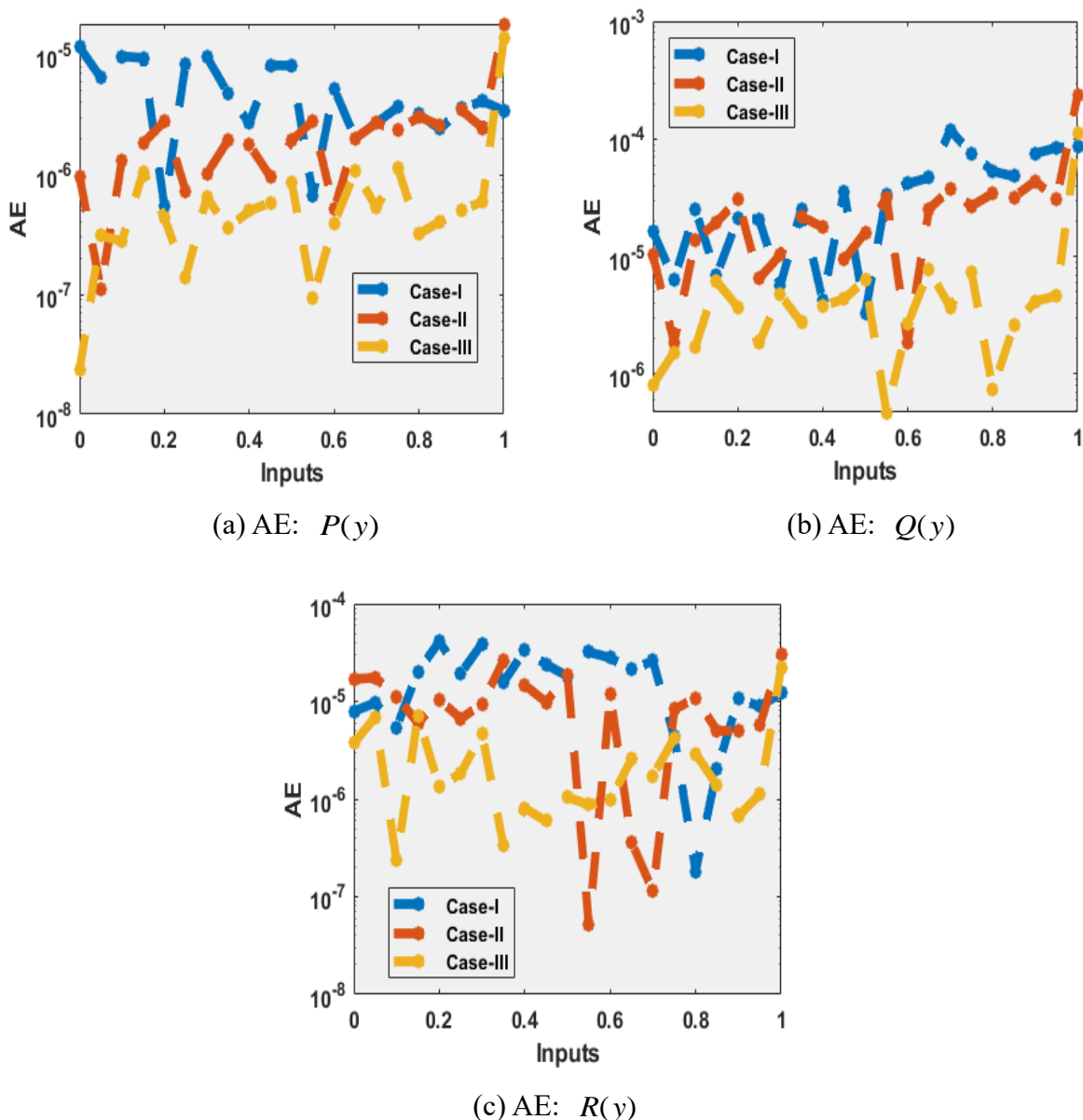


Figure 7. AE values for the predator-prey delay differential system using the ANNs-SCG solve.

5. Conclusions

The aim of the current investigations is to provide the numerical computing performances on the predator-prey delay differential system of Holling form-III. The predator-prey delay form of the differential system with Holling form-III is based on the two delay terms, cooperation/competition dynamics and the prey Allee effects. The competition state helps to induce the instability, whereas the cooperation state makes the stability of the system via Hopf bifurcation. Some concluding remarks of these investigations are presented as:

- A mathematical form of the nonlinear predator-prey model along with the two delay forms of the differential system with Holling form-III is based on the two delay terms, cooperation/competition dynamics and the prey Allee effects.

- The existence of the delay terms in the nonlinear predator-prey model makes more complex. Therefore, the stochastic LVMBPNNs computing procedures is a better way to provide the numerical performances.
- Fifteen numbers of neurons have been applied to solve the predator-prey delay differential system of Holling form-III together with the data selection, which is chosen as 13%, 12% and 75% for testing, training, and substantiation.
- The exactness of the LVMBPNNs computing solver is performed through the comparison of the achieved and reference numerical results.
- The AE measures are calculated in good domains that are found as 10^{-5} to 10^{-8} for each dynamic of the predator-prey delay differential model in Holling form-III.

Upcoming research directions: The designed stochastic procedures can be applied to solve the fluid dynamical systems [46–48], fractional kinds of differential systems [49–53], and nonlinear differential systems [54–56].

Acknowledgments

The research on “Supervised neural learning for the predator-prey delay differential system of Holling form-III” by Khon Kaen University has received funding support from the National Science, Research and Innovation Fund.

Conflict of interest

All authors declare that there are no potential conflicts of interest.

References

1. J. D. Ferreira, C. A. T. Salazar, P. C. C. Tabares, Weak Allee effect in a predator-prey model involving memory with a hump, *Nonlinear Anal.: Real World Appl.*, **14** (2013), 536–548. <https://doi.org/10.1016/j.nonrwa.2012.07.014>
2. M. Cavani, M. Farkas, Bifurcations in a predator-prey model with memory and diffusion. I: Andronov-Hopf bifurcation, *Acta Math. Hung.*, **63** (1994), 213–229. <https://doi.org/10.1007/bf01874129>
3. M. Umar, Z. Sabir, M. A. Z. Raja, Intelligent computing for numerical treatment of nonlinear prey-predator models, *Appl. Soft Comput.*, **80** (2019), 506–524. <https://doi.org/10.1016/j.asoc.2019.04.022>
4. Z. Sabir, T. Botmart, M. A. Z. Raja, W. Weera, An advanced computing scheme for the numerical investigations of an infection-based fractional-order nonlinear prey-predator system, *Plos One*, **17** (2022), 1–13. <https://doi.org/10.1371/journal.pone.0265064>
5. U. Ghosh, S. Pal, M. Banerjee, Memory effect on Bazykin’s prey-predator model: Stability and bifurcation analysis, *Chaos Solitons Fract.*, **143** (2021), 1–10. <https://doi.org/10.1016/j.chaos.2020.110531>
6. A. Gökçe, The influence of past in a population system involving intraspecific competition and Allee effect, *Eur. Phys. J. Plus*, **137** (2022), 1–11. <https://doi.org/10.1140/epjp/s13360-022-02425-z>

7. B. Sahoo, S. Poria, Dynamics of predator-prey system with fading memory, *Appl. Math. Comput.*, **347** (2019), 319–333. <https://doi.org/10.1016/j.amc.2018.11.013>
8. L. Berec, E. Angulo, F. Courchamp, Multiple Allee effects and population management, *Trends Ecol. Evol.*, **22** (2007), 185–191. <https://doi.org/10.1016/j.tree.2006.12.002>
9. B. Souayah, Z. Sabir, M. Umar, M. W. Alam, Supervised neural network procedures for the novel fractional food supply model, *Fractal Fract.*, **6** (2022), 1–15. <https://doi.org/10.3390/fractalfract6060333>
10. E. Angulo, G. M. Luque, S. D. Gregory, J. W. Wenzel, C. Bessa-Gomes, L. Berec, et al., Allee effects in social species, *J. Anim. Ecol.*, **87** (2018), 47–58. <https://doi.org/10.1111/1365-2656.12759>
11. T. Perälä, J. A. Hutchings, A. Kuparinen, Allee effects and the Allee-effect zone in northwest Atlantic cod, *Biol. Lett.*, **18** (2022), 1–6. <https://doi.org/10.1098/rsbl.2021.0439>
12. B. Dennis, Allee effects: Population growth, critical density, and the chance of extinction, *Nat. Resour. Model.*, **3** (1989), 481–538. <https://doi.org/10.1111/j.1939-7445.1989.tb00119.x>
13. T. Botmart, Z. Sabir, M. A. Z. Raja, M. R. Ali, R. Sadat, A. A. Aly, et al., A hybrid swarming computing approach to solve the biological nonlinear Leptospirosis system, *Biomed. Signal Process. Control*, **77** (2022), 103789. <https://doi.org/10.1016/j.bspc.2022.103789>
14. F. Courchamp, L. Berec, J. Gascoigne, *Allee effects in ecology and conservation*, 1 Ed., New York: Oxford University Press Inc., 2008. <https://doi.org/10.1093/acprof:oso/9780198570301.001.0001>
15. C. Çelik, H. Merdan, O. Duman, Ö. Akın, Allee effects on population dynamics with delay, *Chaos Solitons Fract.*, **37** (2008), 65–74. <https://doi.org/10.1016/j.chaos.2006.08.019>
16. J. P. Tripathi, P. S. Mandal, A. Poonia, V. P. Bajjiya, A widespread interaction between generalist and specialist enemies: The role of intraguild predation and Allee effect, *Appl. Math. Model.*, **89** (2021), 105–135. <https://doi.org/10.1016/j.apm.2020.06.074>
17. P. C. Tabares, J. D. Ferreira, V. Rao, Weak Allee effect in a predator-prey system involving distributed delays, *Comput. Appl. Math.*, **30** (2011), 675–699. <https://doi.org/10.1590/S1807-03022011000300011>
18. T. Botmart, W. Weera, Guaranteed cost control for exponential synchronization of cellular neural networks with mixed time-varying delays via hybrid feedback control, *Abstr. Appl. Anal.*, **2013** (2013), 175796. <https://doi.org/10.1155/2013/175796>
19. M. Jovanović, M. Krstić, Extinction in stochastic predator-prey population model with Allee effect on prey, *Discrete Cont. Dyn. Syst. Ser. B*, **22** (2017), 2651–2667. <https://doi.org/10.3934/dcdsb.2017129>
20. P. J. Pal, T. Saha, M. Sen, M. Banerjee, A delayed predator–prey model with strong Allee effect in prey population growth, *Nonlinear Dyn.*, **68** (2012), 23–42. <https://doi.org/10.1007/s11071-011-0201-5>
21. A. Surendran, M. J. Plank, M. J. Simpson, Population dynamics with spatial structure and an Allee effect, *Proc. Math. Phys. Eng. Sci.*, **476** (2020), 20200501. <https://doi.org/10.1098/rspa.2020.0501>
22. M. Jankovic, S. Petrovskii, Are time delays always destabilizing? Revisiting the role of time delays and the Allee effect, *Theor. Ecol.*, **7** (2014), 335–349. <https://doi.org/10.1007/s12080-014-0222-z>

23. A. W. Stoner, M. Ray-Culp, Evidence for Allee effects in an over-harvested marine gastropod: Density-dependent mating and egg production, *Mar. Ecol. Prog. Ser.*, **202** (2000), 297–302. <http://dx.doi.org/10.3354/meps202297>
24. F. Courchamp, B. T. Grenfell, T. H. Clutton-Brock, Impact of natural enemies on obligately cooperative breeders, *Oikos*, **91** (2000), 311–322. <https://doi.org/10.1034/j.1600-0706.2000.910212.x>
25. M. Kuussaari, I. Saccheri, M. Camara, I. Hanski, Allee effect and population dynamics in the Glanville fritillary butterfly, *Oikos*, **82** (1998), 384–392. <https://doi.org/10.2307/3546980>
26. Z. Ma, Hopf bifurcation of a generalized delay-induced predator-prey system with habitat complexity, *Int. J. Bifurcat. Chaos*, **30** (2020), 2050082. <https://doi.org/10.1142/S0218127420500820>
27. H. Yu, M. Zhao, R. P. Agarwal, Stability and dynamics analysis of time delayed eutrophication ecological model based upon the Zeya reservoir, *Math. Comput. Simul.*, **97** (2014), 53–67. <https://doi.org/10.1016/j.matcom.2013.06.008>
28. Y. Tang, L. Zhou, Stability switch and Hopf bifurcation for a diffusive prey–predator system with delay, *J. Math. Anal. Appl.*, **334** (2007), 1290–1307. <https://doi.org/10.1016/j.jmaa.2007.01.041>
29. A. Gökçe, A mathematical study for chaotic dynamics of dissolved oxygen-phytoplankton interactions under environmental driving factors and time lag, *Chaos Solitons Fract.*, **151** (2021), 1–13. <https://doi.org/10.1016/j.chaos.2021.111268>
30. K. Chakraborty, M. Chakraborty, T. K. Kar, Bifurcation and control of a bioeconomic model of a prey–predator system with a time delay, *Nonlinear Anal.: Hybrid Syst.*, **5** (2011), 613–625. <https://doi.org/10.1016/j.nahs.2011.05.004>
31. H. Zhao, X. Huang, X. Zhang, Hopf bifurcation and harvesting control of a bioeconomic plankton model with delay and diffusion terms, *Phys. A: Stat. Mech. Appl.*, **421** (2015), 300–315. <https://doi.org/10.1016/j.physa.2014.11.042>
32. A. Gökçe, Numerical bifurcation analysis for a prey-predator type interactions with a time lag and habitat complexity, *Bitlis Eren Üniv. Fen Bilim. Derg.*, **10** (2021), 57–66. <https://doi.org/10.17798/bitlisfen.840245>
33. K. Gopalsamy, G. Ladas, On the oscillation and asymptotic behavior of $\dot{N}(t) = N(t)[a + bN(t - \tau) - cN^2(t - \tau)]$, *Quart. Appl. Math.*, **48** (1990), 433–440.
34. M. Umar, Z. Sabir, F. Amin, J. L. Guirao, M. A. Z. Raja, Stochastic numerical technique for solving HIV infection model of CD4+ T cells, *Eur. Phys. J. Plus*, **135** (2020), 1–19. <https://doi.org/10.1140/epjp/s13360-020-00417-5>
35. Z. Sabir, Stochastic numerical investigations for nonlinear three-species food chain system, *Int. J. Biomath.*, **15** (2022), 2250005. <https://doi.org/10.1142/S179352452250005X>
36. Z. Sabir, M. R. Ali, R. Sadat, Gudermannian neural networks using the optimization procedures of genetic algorithm and active set approach for the three-species food chain nonlinear model, *J. Ambien. Intell. Human. Comput.*, **13** (2022), 1–10. <https://doi.org/10.1007/s12652-021-03638-3>
37. M. Umar, Z. Sabir, M. A. Z. Raja, M. Shoaib, M. Gupta, Y. G. Sánchez, A stochastic intelligent computing with neuro-evolution heuristics for nonlinear SITR system of novel COVID-19 dynamics, *Symmetry*, **12** (2020), 1–17. <https://doi.org/10.3390/sym12101628>
38. M. Umar, F. Amin, H. A. Wahab, D. Baleanu, Unsupervised constrained neural network modeling of boundary value corneal model for eye surgery, *Appl. Soft Comput.*, **85** (2019), 1–16. <https://doi.org/10.1016/j.asoc.2019.105826>

39. B. Wang, J. F. Gomez-Aguilar, Z. Sabir, M. A. Z. Raja, W. F. Xia, H. Jahanshahi, et al., Numerical computing to solve the nonlinear corneal system of eye surgery using the capability of Morlet wavelet artificial neural networks, *Fractals*, **30** (2022), 1–19. <https://doi.org/10.1142/S0218348X22401478>
40. Z. Sabir, Neuron analysis through the swarming procedures for the singular two-point boundary value problems arising in the theory of thermal explosion, *Eur. Phys. J. Plus*, **137** (2022), 1–18. <https://doi.org/10.1140/epjp/s13360-022-02869-3>
41. Z. Sabir, H. A. Wahab, Evolutionary heuristic with Gudermannian neural networks for the nonlinear singular models of third kind, *Phys. Scr.*, **96** (2021), 1–12. <https://doi.org/10.1088/1402-4896/ac3c56>
42. T. Saeed, Z. Sabir, M. S. Alhodaly, H. H. Alsulami, Y. G. Sánchez, An advanced heuristic approach for a nonlinear mathematical based medical smoking model, *Results Phys.*, **32** (2022), 1–13. <https://doi.org/10.1016/j.rinp.2021.105137>
43. A. Gökçe, A dynamic interplay between Allee effect and time delay in a mathematical model with weakening memory, *Appl. Math. Comput.*, **430** (2022), 127306. <https://doi.org/10.1016/j.amc.2022.127306>
44. M. R. Ali, S. Raut, S. Sarkar, U. Ghosh, Unraveling the combined actions of a Holling type III predator–prey model incorporating Allee response and memory effects, *Comp. Math. Methods.*, **3** (2021), 1–18. <https://doi.org/10.1002/cmm4.1130>
45. A. Rojas-Palma, E. González-Olivares, Optimal harvesting in a predator-prey model with Allee effect and sigmoid functional response, *Appl. Math. Model.*, **36** (2012), 1864–1874. <https://doi.org/10.1016/j.apm.2011.07.081>
46. T. Botmart, N. Yotha, P. Niamsup, W. Weera, Hybrid adaptive pinning control for function projective synchronization of delayed neural networks with mixed uncertain couplings, *Complexity*, **2017** (2017), 4654020. <https://doi.org/10.1155/2017/4654020>
47. P. Lakshminarayana, K. Vajravelu, G. Sucharitha, S. Sreenadh, Peristaltic slip flow of a Bingham fluid in an inclined porous conduit with Joule heating, *Appl. Math. Nonlinear Sci.*, **3** (2018), 41–54. <https://doi.org/10.21042/AMNS.2018.1.00005>
48. T. Sajid, S. Tanveer, Z. Sabir, J. L. G. Guirao, Impact of activation energy and temperature-dependent heat source/sink on Maxwell–Sutterby fluid, *Math. Probl. Eng.*, **2020** (2020), 1–15. <https://doi.org/10.1155/2020/5251804>
49. R. Ahmad, A. Farooqi, J. Zhang, N. Ali, Steady flow of a power law fluid through a tapered non-symmetric stenotic tube, *Appl. Math. Nonlinear Sci.*, **4** (2019), 255–266. <https://doi.org/10.2478/AMNS.2019.1.00022>
50. Z. Sabir, A. Imran, M. Umar, M. Zeb, M. Shoaib, M. A. Z. Raja, A numerical approach for 2-D Sutterby fluid-flow bounded at a stagnation point with an inclined magnetic field and thermal radiation impacts, *Therm. Sci.*, **25** (2021), 1975–1987. <https://doi.org/10.2298/TSCI191207186S>
51. Z. Sabir, M. A. Z. Raja, M. Shoaib, J. F. Aguilar, FMNEICS: Fractional Meyer neuro-evolution-based intelligent computing solver for doubly singular multi-fractional order Lane–Emden system, *Comp. Appl. Math.*, **39** (2020), 1–18. <https://doi.org/10.1007/s40314-020-01350-0>
52. H. Günerhan, E. Çelik, Analytical and approximate solutions of fractional partial differential-algebraic equations, *Appl. Math. Nonlinear Sci.*, **5** (2020), 109–120. <https://doi.org/10.2478/amns.2020.1.00011>

53. K. A. Touchent, Z. Hammouch, T. Mekkaoui, A modified invariant subspace method for solving partial differential equations with non-singular kernel fractional derivatives, *Appl. Math. Nonlinear Sci.*, **5** (2020), 35–48. <https://doi.org/10.2478/amns.2020.2.00012>
54. Z. Sabir, M. A. Z. Raja, J. L. Guirao, T. Saeed, Meyer wavelet neural networks to solve a novel design of fractional order pantograph Lane-Emden differential model, *Chaos Solitons Fract.*, **152** (2021), 1–14. <https://doi.org/10.1016/j.chaos.2021.111404>
55. E. İlhan, İ. O. Kıymaz, A generalization of truncated M-fractional derivative and applications to fractional differential equations, *Appl. Math. Nonlinear Sci.*, **5** (2020), 171–188. <https://doi.org/10.2478/amns.2020.1.00016>
56. H. M. Baskonus, H. Bulut, T. A. Sulaiman, New complex hyperbolic structures to the lonngren-wave equation by using sine-gordon expansion method, *Appl. Math. Nonlinear Sci.*, **4** (2019), 129–138. <https://doi.org/10.2478/AMNS.2019.1.00013>



AIMS Press

© 2022 the Author(s), licensee AIMS Press. This is an open access article distributed under the terms of the Creative Commons Attribution License (<http://creativecommons.org/licenses/by/4.0>)